On the influence of the Sun on the rapid variability of compact extragalactic sources

N. Marchili[1], T. P. Krichbaum[1], X. Liu[2], H.-G. Song[2], J. M. Anderson[1], A. Witzel[1], and J. A. Zensus[1]

[1] Max-Planck-Institut für Radioastronomie, Auf dem Hügel 69, 53121 Bonn, Germany
e-mail: marchili@mpifr-bonn.mpg.de
[2] Urumqi Observatory, the National Astronomical Observatories, the Chinese Academy of Sciences, Urumqi 830011, PR China

ABSTRACT

Starting from December 2004, a program for the monitoring of intraday variable sources at a frequency of 5 GHz was performed at the Urumqi Observatory. The analysis of the variability characteristics of the flat-spectrum radio source AO 0235+164 revealed the existence of an annual cycle in the variability amplitude. This appears to correlate with the solar elongation of the source. A thorough analysis of the results of the MASIV IDV survey — which provides the variability characteristics of a large sample of compact radio sources — confirms that there is a small but detectable component of the observed fractional modulation which increases with decreasing solar elongation. We discuss the hypothesis that the phenomenon is related to interplanetary scintillation.

Key words. scattering; quasars: individual: AO 0235+164; radio continuum: galaxies; solar wind

1. Introduction

IntraDay Variability (IDV, see Witzel et al. 1986, Heeschen et al. 1987) refers to the fast intensity variability — on time scales from a few hours to ~ 2 days — which affects a considerable number of flat-spectrum radio sources (a fraction between 30% and 50%, see Quirrenbach et al. 1992 and Lovell et al. 2008). The variability concerns both total flux density and polarization measurements over a wide range of the electromagnetic spectrum, from the radio to the optical bands.

Both source-intrinsic and source-extrinsic models have been proposed in order to explain IDV. In the optical bands, the variability should be regarded as intrinsic to the sources (Wagner & Witzel 1995). Concerning the radio bands, the problem of the origin of the variability is not yet solved. For the most extreme sources — the so-called fast-scintillators (see Dennett-Thorpe & de Bruyn 2002, Bignall et al. 2003), which show total flux variations of the order of 100% on time scales of hours — the variability is most likely due to InterStellar Scintillation (ISS), caused by nearby scattering screens located at a distance of several parsecs (see Dennett-Thorpe & de Bruyn 2002, Rickett et al. 2006). However, only a very small fraction of IDV sources can be labeled as fast scintillators. In the Micro-Arcsecond Scintillation-Induced Variability (MASIV) survey (Lovell et al. 2003 and 2008), a strong correlation was found between the variability amplitude of a large sample of compact radio sources and the emission measure in the ionized interstellar medium along their respective lines of sight, showing that a significant part of the variability is due to ISS.

The discovery of correlated variations in the optical and radio light curves of S5 0716+714 (Quirrenbach et al. 1991) suggested that at least part of its variability is intrinsic to the source. This gives rise to the fundamental issue to establish how large the contribution of source-intrinsic mechanisms to the to-tal variability is and, even more important, whether the case of S5 0716+714 should be regarded as an exception among IDV sources.

A possible way to investigate the nature of IDV in a given source is to study how its variability characteristics, namely amplitude and time scale, change with time. Following Narayan 1992, we shortly discuss how these quantities vary in case of IDV which is caused by ISS. They can both be described in terms of the Fresnel scale, r_{f}, and the diffraction scale, r_{diff}. The former is given by $r_{\mathrm{f}} \sim \sqrt{\lambda D}$, where D is the distance between the observer and the scattering screen. The latter depends on the properties of the screen and the wavelength of the observations; concerning the interstellar medium, typical values of r_{f} are of the order of 10^{10} cm for observations at centimeter wavelengths and screen distances of the order of 10-100 pc. In case the variability is caused by weak scattering — as one would expect for classical IDV radio sources — and the angular source size θ_{s} is larger than the Fresnel angle $\theta_{\mathrm{f}} = r_{\mathrm{f}}/D$, the characteristic variability time scale can be expressed as

$$\tau_{\mathrm{c}} \approx \frac{r_{\mathrm{f}}}{v}\frac{\theta_{\mathrm{s}}}{\theta_{\mathrm{f}}} \tag{1}$$

where v is the relative velocity between the screen and the observer.

For a given time series, a measure of its variability amplitude is given by the modulation index, m_{i}, which is the ratio of the standard deviation to the average. In case of ISS-originated variability, the modulation index of a light curve is given by Narayan (1992) as

$$m_{\mathrm{i}} \approx \left(\frac{r_{\mathrm{f}}}{r_{\mathrm{diff}}}\right)^{5/6}\left(\frac{\theta_{\mathrm{f}}}{\theta_{\mathrm{s}}}\right)^{7/6} \tag{2}$$

The two equations above can be used to predict how the variability characteristics of a source should evolve throughout the year. The time scale of scintillation-induced variability changes

---
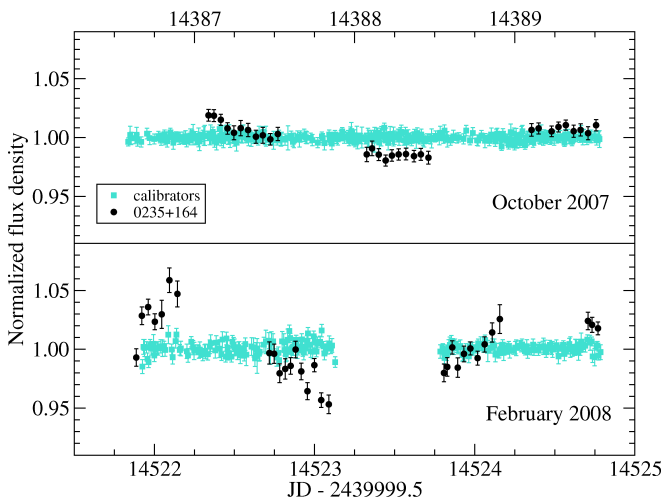
Fig. 1. The variability curves of AO 0235+164 (black dots) in October 2007 (upper panel) and February 2008 (lower panel), examples, respectively, of a low and a high variability state of the source.

Fig. 2. Solar elongation (upper panel) and modulation index (lower panel) of AO 0235+164 plotted versus observing time. The orange line shows the sum of the three variability components which correspond to the harmonics of the signal highlighted in the periodogram analysis in Fig. 3. The cyan line shows a sinusoidal fit obtained after removing the data-points corresponding to the two epochs at smallest solar elongation.

with the relative velocity between the scattering screen and the observer. Due to the Earth's motion around the Sun, this velocity follows an annual cycle which should result in an annual modulation of the variability time scale (see Dennett-Thorpe & de Bruyn 2000, Rickett et al. 2001, Gabányi et al. 2007). The modulation index, instead, should not change with time, unless the variability time scale exceeds the total duration of the observations, in which case the detected variability would decrease as the time scale increases.
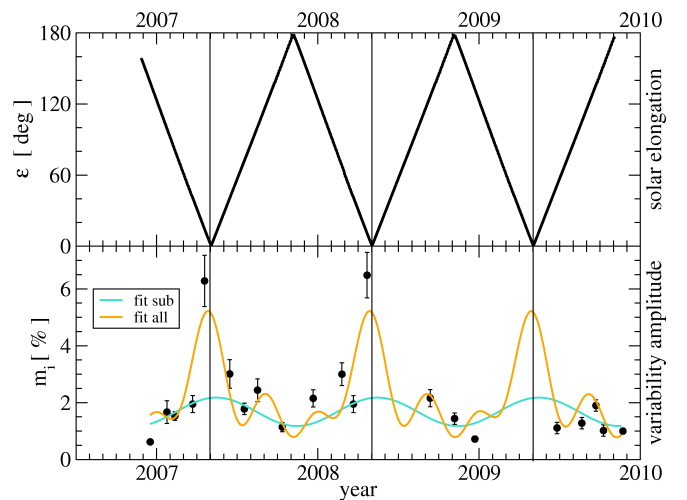
In 2004, a collaboration between the Max-Planck-Institut für Radioastronomie (MPIfR) and the Urumqi Observatory initiated a project for the monitoring of classical IDV sources (Gabányi et al. 2007, Marchili et al. 2008 and 2010). The aim of the project is to study how the variability characteristics of the target sources change with time. Among others, a sample of 6 well known IDV sources has been regularly observed with the 25m-Urumqi radio telescope, at a frequency of 4.80 GHz. These are the flat-spectrum radio sources AO 0235+164, 0716+714, 0917+624, 0954+658, 1128+592 and 1156+295. The project is still ongoing; through February 2010, 42 observing sessions were carried out. The main characteristics of the 21 epochs in which AO 0235+164 was observed are summarized in Table 1: in Col. 1 we report the observing date at half-session, in Col. 2 the corresponding day (0=January 1st, 2005), in Col. 3 the duration of the observations, in Col. 4 the number of observed sources (including the calibrators) and in Col. 5 the duty cycle (i.e. the average number of data-points per source per hour).

2. Urumqi data

2.1. Observation and data calibration

The observations have been performed with the 25-meter parabolic antenna of the Nanshan radio telescope, operated by the Urumqi Observatory (for more details, see Sun et al. 2006, Marchili et al. 2010 and references therein). Its single beam dual polarization receiver, built by the MPIfR, is centered at a frequency of 4.80 GHz and has a bandwidth of 600 MHz.

All the flux density measurements have been performed in cross-scan mode, each scan consisting of 8 sub-scans — 4 in azimuth, 4 in elevation — over the source position. This ob-

serving mode allows the evaluation and correction of residual small pointing offsets and the detection of non-Gaussian cross-scan profiles in case of in-beam confusion.

The data calibration procedure follows a standard pipeline. A Gaussian fit to the sub-scans provides an estimate of the flux density. After a quality check, an error-weighted average on the reliable sub-scans provides a flux density measurement for each scan. This value is then corrected for the antenna-gain dependency on both the elevation and the weather conditions, by parameterizing the changes that these effects induce on several calibrators. The accuracy in the flux density measurements can be evaluated through the modulation index of the calibrators, m_0. During normal weather conditions, we find m_0 values between 0.5 and 0.7%. A more thorough description of the data calibration procedure can be found in Kraus (1997), Marchili (2009) and references therein.

2.2. Variability characteristics of AO 0235+164

The flat-spectrum radio source AO 0235+164 (z=0.94) was found to show variability on IDV time scales more than once in the past (see, e.g., Kraus et al. 1999); Senkbeil et at. (2008) reported a likely extreme-scattering-event in AO 0235+164 in July 2005. The source was observed with the Urumqi radio telescope in 21 epochs between December 2006 and November 2009. Two of the collected light curves are shown in Fig. 1. In Table 1, for each observing session we summarize the calibration accuracy (m_0; Col. 6) and the variability amplitude of AO 0235+164 (Col. 7) in terms of the modulation index m_i. The uncertainties on m_i — evaluated by means of synthetic light curves having the same sampling as the original curves — range between 10 and 20% of the m_i estimations.

Table 1. The observing sessions of the Urumqi monitoring program in which AO 0235+164 was observed.

Epoch	Day	Duration (d)	N. S.	Duty cycle (data h^{-1})	m_0 (%)	m_i (%)
2006.12.18	718	2.4	12	1.3	0.6	0.62
2007.01.25	755	2.3	14	1.1	0.7	1.67
2007.02.12	773	4.0	15	1.0	0.6	1.53
2007.03.24	813	2.8	16	0.9	0.7	1.95
2007.04.20	840	3.7	16	0.8	0.8	6.28
2007.06.16	897	2.4	16	0.9	0.7	3.01
2007.07.19	930	2.9	18	0.9	0.7	1.78
2007.08.18	960	3.1	15	1.0	0.8	2.44
2007.10.13	1016	3.0	16	0.8	0.5	1.14
2007.12.22	1086	3.2	15	1.0	0.5	2.15
2008.02.25	1151	2.9	15	0.8	0.6	3.00
2008.03.22	1177	3.0	15	1.1	0.5	1.95
2008.04.22	1208	3.1	14	0.9	0.5	6.48
2008.09.12	1351	3.5	14	1.1	0.5	2.16
2008.11.06	1406	3.6	15	0.5	0.7	1.44
2008.12.22	1452	2.4	15	1.0	0.5	0.72
2009.06.26	1638	2.6	16	0.7	0.5	1.11
2009.08.21	1694	4.1	16	0.9	0.5	1.28
2009.09.22	1726	5.5	14	0.9	0.5	1.90
2009.10.09	1743	2.3	15	1.1	0.5	1.02
2009.11.22	1787	3.8	16	0.8	0.6	1.00
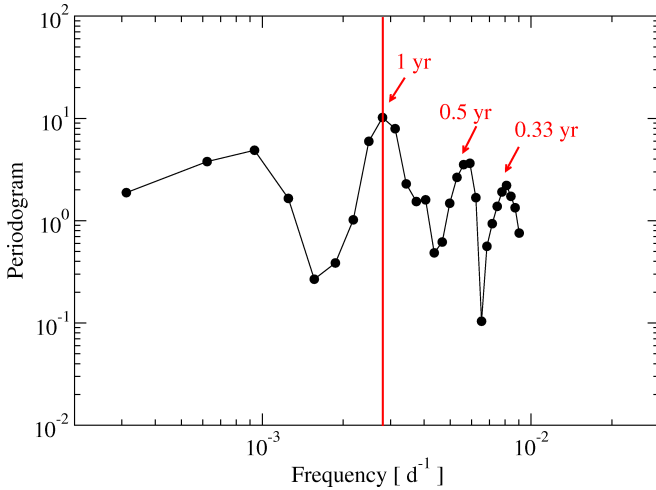
Fig. 3. Periodogram analysis of the variability amplitudes m_i of AO 0235+164. Four peaks of power are clearly visible; three of them correspond to periods of 1, 1/2 and 1/3 of year (red arrows), i.e. the first three harmonics of a 1-year periodic signal. This is strong evidence in favour of an annual cycle in the variability amplitude of the source.

2.3. Annual variation in the modulation index of AO 0235+164

Plotting m_i versus the date of the observation, it appears that the modulation index of AO 0235+164 (black dots in Fig. 2, lower panel) follows a regular pattern. The variability seems to be more intense between February and August, weaker between September and January. To investigate this effect, we applied to m_i a Lomb-Scargle periodogram analysis (see Lomb 1976, Scargle 1982), which highlighted the existence of a periodic oscillation with a period of one year (see Fig. 3).

We summed up the variability components corresponding to the three harmonics of the signal which are indicated in the periodogram analysis in Fig. 3. This allows an estimate of the

amplitude and phase of the periodic oscillation. The annual cycle (orange line in Fig. 2, lower panel) peaks at the time of the year in which the solar elongation of AO 0235+164, ϵ_{0235}, is at the minimum (see Fig. 2, upper panel). The yearly variation observed in m_i has a high amplitude in 2007 and 2008. In 2009, the modulation is not clearly visible. This may be due to the lack of observations between January and July, which is the time span in which we would expect the largest variations. However, we may notice that between 2008 and 2009 the solar activity was very low, due to the transition from the 23rd to the 24th solar cycle. In this sense, the absence of significant changes in the variability amplitude of AO 0235+164 may support the hypothesis that these changes are related to the solar activity and therefore are induced by the Sun.

Two measurements of m_i stand out from the others; they correspond to the observing sessions performed in April 2007 and April 2008. In those epochs, the solar elongation ϵ_{0235} was relatively small ($\sim 13°$ and $\sim 11°$, respectively). We repeated the periodogram analysis excluding the two data-points with $\epsilon_{0235} < 30°$, in order to establish if the increase of the m_i value is limited to the sole epochs of small solar elongation. We found that a periodic oscillation with period of about one year is still clearly detectable. A sinusoidal fit to these data (see Fig. 2, lower panel, cyan line) shows that the oscillation has a peak-to-peak amplitude of $\sim 1.1\%$, while the average m_i value is $\sim 1.7\%$. The increase in m_i between the time of maximum and minimum solar elongation is of the order of 90%. This implies that, during our observations, the solar elongation plays the main role in the variability of AO 0235+164. The phase of the periodic signal is slightly offset (~ 10 days) with respect to the time of the year of minimum elongation. This offset, however, is much smaller than the average time separation between consecutive observing sessions (~ 50 days). We can conclude that periodic variations correlated to solar elongation affect the modulation index of AO 0235+164 even for solar elongation ϵ_{0235} larger than 30°.
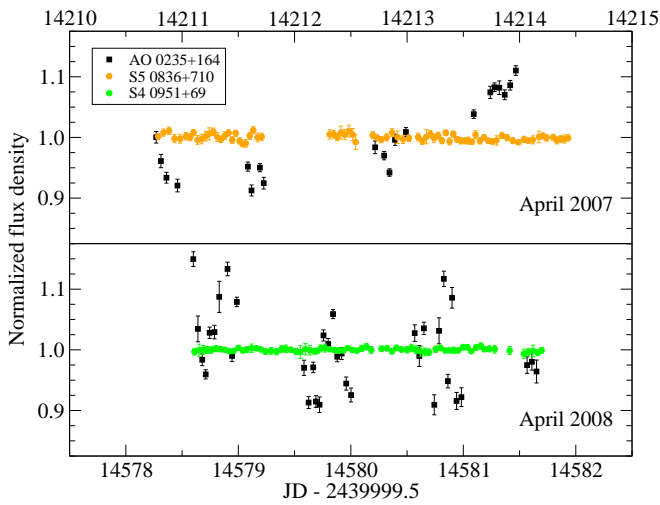
2.4. Variability time scale

At first sight, one may think that the existence of an annual cycle in the modulation index of an IDV source may be related to an annual modulation in its variability time scales. As explained above, m_i could undergo yearly-periodic changes if the variability time scale exceeds the duration of the observations. In this case, the variations in τ_c and m_i should be anti-correlated. We can check this hypothesis by studying how τ_c changes as a function of m_i. For each observing session, we estimated the characteristic variability time scale of AO 0235+164 by applying to the light curves three different kinds of time analysis methods, namely a first-order structure function analysis (see Simonetti et al. 1985), a wavelet-based algorithm (Marchili et al., in prep.) and a sinusoidal fitting procedure. The uncertainties in the time scales are mostly due to the limited duration of the observations, obs_d. We estimated them as proportional to $(\tau_c^{3/2})/(obs_d)^{1/2}$. The proportionality factor has been calculated by looking at the distribution of the peak-to-peak time scale — the time interval between a local minimum (or maximum) and the following maximum (or minimum) — for a few light curves characterized by fast variability.

In Fig. 4 we plot the variability time scales versus m_i for all the epochs in which the source showed significant variability (i.e. the probability of constant flux density was lower than 0.1%, according to a chi-square test). A cycle in m_i as strong as the one we observed in AO 0235+164 should result in a clear increase of τ_c as m_i decreases. The plot, however, does not reveal such
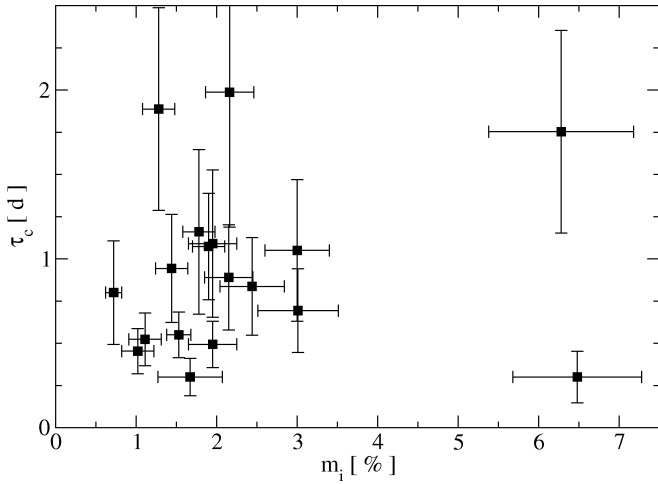
Fig. 4. The variability time scales of AO 0235+164 plotted versus m_i.

Fig. 5. The variability curves of AO 0235+164 (black squares) in April 2007 (upper panel) and April 2008 (lower panel), compared with the curves of the calibrators S5 0836+710 (orange dots) and S4 0951+69 (green dots). The time scale of the variability in the two epochs is considerably different.

a trend. In particular, while the extreme variability observed in April 2007 is characterized by a value of τ_c among the highest detected in the source, the one for the April 2008 observations is quite low (see Fig. 5). This leads to the conclusion that the annual cycle in m_i cannot be explained in terms of an annual modulation of the variability time scale.

3. MASIV data

Given the large number of sources it comprises, the MASIV survey seems to be the ideal test ground to further investigate the possible correlation between the variability characteristics of compact radio sources and their solar elongation.

MASIV is a survey of 710 radio sources, undertaken at a frequency of 4.9 GHz at the Very Large Array (VLA) between January 2002 and January 2003. The main aim of the project was to provide a large sample of scintillating sources for reliable statistical investigation. A core sample of 578 sources was observed in four epochs of 3 or 4 days duration, starting on 2002 January 19, May 9, September 13 and 2003 January 10. The results of

these observations, along with a detailed description of the observing strategy and data calibration, are reported in Lovell et al. (2008). After removal of the sources which show structure on VLA arcsecond scales or are partially resolved, 475 point sources were left. Basic information about the sources, their flux density and the raw modulation index for each of the four epochs are provided by Lovell et al. (2008), and are available in the electronic edition of the *Astrophysical Journal*.

We used the modulation indices resulting from the MASIV survey to check whether the data support the hypothesis of an additional contribution to the variability, related to solar elongation. We also checked whether such an effect depends on the ecliptic latitude of the sources, as it would be reasonable to expect.

3.1. Modulation index variations as a function of solar elongation

We labeled the four epochs of MASIV observation chronologically, as t_j {j=1,..., 4}. For each session and source, we calculated the solar elongation $\epsilon_{src,j}$. We also defined a new parameter, the fractional modulation index, as

$$fm_{src,\,j} = \frac{m_{src,\,j}}{<m_{src}>} \qquad (3)$$

where $m_{src,\,j}$ is the modulation index at the epoch t_j and $<m_{src}>$ is the average modulation index over the four observing sessions. By means of the fractional modulation index, we can compare the changes in the variability amplitude of sources with very different variability characteristics. In a statistical approach, the fm values have been combined, in order to study how the variability amplitude changes, on average, as a function of ϵ. We excluded from the analysis the light curves which have been used to calibrate the data (H. Bignall, priv. comm.), because their modulation index is artificially low.

If the effect observed in AO 0235+164, described above, is common to compact extragalactic sources, we expect to see an increase in fm as ϵ approaches zero. At first sight, the scattering in the individual fm values is too high to reveal a clear trend. A 60-point running average over the data (see Fig. 6, black line) demonstrates the existence of such an increase. In cyan dots, we also plotted the 5-degree average, which confirms the behaviour of the running average. The averaged fm peaks at $\epsilon \sim 10°$ with a value of ~ 1.25, while the minimum falls close to $\epsilon \sim 165°$ with a value of ~ 0.9. Most remarkably, all the averaged fm values for $\epsilon < 35°$ are $\gtrsim 1.15$, while for $\epsilon > 110°$ most of the values are < 1.0. We conclude that solar elongation exerts a considerable influence on the variability of compact radio sources.

Concerning the MASIV survey, the contribution of the solar-elongation related effect to the total variability should not have very serious implications for its main findings. In particular, all the results obtained by using the structure function at a time lag of two days ($D(2$ days) in Lovell et al. 2008) as an estimate of the source variability should be only marginally affected. This is because $D(2$ days) is calculated over all the four observing sessions. Based on Fig. 6, given a 30-40% enhancement in the modulation index between maximum and minimum solar elongation, the additional contribution from the solar elongation effect to the 4-epoch combined variability would be of the order of 10% of the total fractional variation for sources observed at low solar elongations.
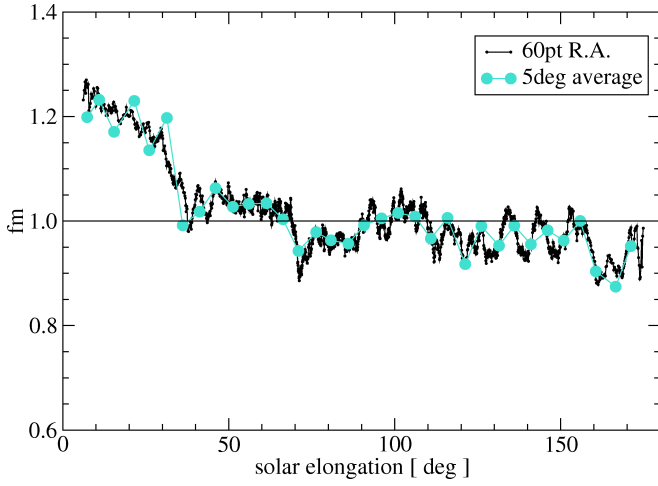
Fig. 6. Results of a 60-point running average on the combined fractional modulation index of MASIV sources (black line) plotted versus solar elongation. The cyan dots show a 5-degree average. The increase in the variability amplitude for $\epsilon < 30°$ is remarkable.

3.2. Dependence on ecliptic latitude

A solar elongation related effect should be particularly strong for sources at low ecliptic latitude, due to the large solar elongation range they cover. Let us define ϵ_{min} and ϵ_{max} as the minimum and maximum solar elongation for a given source during the year. We would expect $m_i(\epsilon_{min}) - m_i(\epsilon_{max})$ (from now on, Δm_{max}) to increase as the ecliptic latitude β tends to zero. In order to verify the hypothesis, for each source in the MASIV catalogue we applied a linear regression to the four m_i values as a function of ϵ. The regression coefficient A has been used to estimate the variation in the modulation index, as follows:

$$\Delta m_{max} = A \left(\epsilon_{min} - \epsilon_{max} \right) \tag{4}$$

The Δm_{max} values obtained for all sources, averaged in bins of 2 (black dots) and 5 degrees (orange dots), are presented in Fig. 7. Δm_{max} is clearly β-dependent. For sources at $\beta \sim 0°$, Δm_{max} is of the order of 100%. It decreases on both sides of the β axis, till it reaches a value close to 0% at $\beta \sim 30°$.

The calculation of the mean fractional modulation index values at different epochs reveals an interesting characteristic. The averages for the January 2002 and 2003 epochs are systematically smaller than for May and September 2002. The measured values are shown in Table 2 (Col. 2). This result needs to be carefully examined. The distribution of the sources as a function of solar elongation changes during the year. In January the Sun is at low declination. Since the MASIV survey includes only sources above declination 0°, in January the average solar elongation is considerably higher than in May and September. As a consequence, a systematic bias in the measured modulation indices at different epochs — whatever the cause — could in principle fake a solar elongation dependence of the variability. Viceversa, a solar elongation dependence of the variability would affect the average modulation indices measured at different times of the year. If the first hypothesis is correct, the average values of fm should not depend on β. If the second hypothesis is correct, the differences in fm at different epochs should be very pronounced for sources at low β, negligible for the ones at high β.

The fm averages for two subsamples of sources at low ($< 15°$) and high ($> 45°$) ecliptic latitude are reported in Table 2, Col. 3 and 4 respectively.
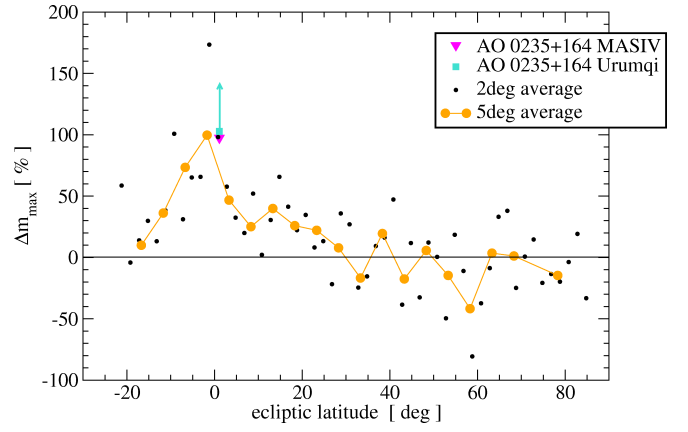
Fig. 7. The modulation index change, Δm_i, as a source passes from the farthest to the closest point to the Sun plotted versus ecliptic latitude β. The 2-degree (black dots) and 5-degree average (orange dots) pinpoint the large increase in variability for sources with low β. The variation deduced from Urumqi observation for AO 0235+164, plotted as a cyan square, has been obtained excluding the April 2007 and April 2008 observations, and should be regarded as a lower limit.

Table 2. The mean fractional modulation index of the four MASIV observing sessions. The average fractional modulation index is compared with the averages for the subsamples of source with $|\beta| < 15°$ and $|\beta| > 45°$.

Epoch	fm	$fm(|\beta| < 15°)$	$fm(|\beta| > 45°)$
January 2002	0.92	0.85	1.04
May 2002	1.10	1.18	1.03
September 2002	1.11	1.17	1.05
January 2003	0.87	0.80	0.88

It appears that the fractional modulation index is strongly β-dependent even within a single observing session, which confirms the existence of a solar-elongation related effect. The similarity between the averages at high β for January, May, and September 2002 seem to indicate that the low average fm value in January 2002 is mainly due to solar elongation. In the case of January 2003, instead, the low fm values at both low and high β cannot be solely ascribed to a solar elongation effect.

We compared the fm averages in Col. 2 of Table 2 with the number of variable sources, N_{var}, detected in each epoch, reported in Fig. 5 of Lovell et al. 2008. N_{var} increases by $\sim 20\%$ from January 2002 to May, by a few percent from May to September and decreases of $\sim 25 - 30\%$ from September to January 2003. This is in excellent agreement with the behaviour of the fm averages, confirming that the solar-elongation related effect significantly contributes to the variability observed in MASIV sources.

3.3. Comparison between MASIV and Urumqi results

We compared the results obtained from the MASIV sample with the ones from the Urumqi observations. AO 0235+164 has an ecliptic latitude $\beta \sim 1°$; it was observed both in the MASIV survey and in the Urumqi IDV monitoring project. In the first case, we find a Δm_{max} value of 97% (plotted in Fig. 7 as a purple triangle), in excellent agreement with the sources-averaged Δm_{max} at $\beta \sim 0°$, which is 98%. If we calculate in a similar way the Δm_{max} for the Urumqi observations (cyan square in Fig. 7), we

find values which range from ∼ 90 to almost 400%, depending on whether the April 2007 and 2008 epochs are excluded from the calculation or not. The exceptional increase in the variability observed in Urumqi for $\epsilon \sim 10°$ finds no confirmation in the observations of AO 0235+164 in the May epoch of MASIV, when the solar elongation of the source was below 10°.

4. Discussion

The combined analysis of Urumqi and MASIV results has provided enough evidence to claim the existence of a source of variability which is related to solar elongation. The nature of the variability, however, is not yet clear. Below, some possible explanations are proposed. The discussion of the different models is based on the results of the Urumqi observations, for which we could estimate both the amplitude and the time scales of the variability.

4.1. Weak scattering

Assuming that the variability is caused by weak scattering, we can use Eq. 1 and 2 to figure out what conditions would be needed to match the variability characteristics we observed — namely, $m_i \sim 1$–10% and $\tau_c \sim 10^4$–10^5 s. Assuming a scattering screen at 1 a.u. distance, we can calculate a Fresnel scale $r_f \sim 10^2$ km and a Fresnel angle $\theta_f \sim 10^2$ mas. The only parameters we can modify to obtain the proper time scale are the angular size of the emitting region θ_s and the relative velocity between the screen and the observer, v.

Setting a velocity of the order of the solar wind speed ($\sim 10^2$ km s^{-1}) would lead to $\theta_s \geq 10^4 \theta_f$, which means 100″ at least. Looking at the full-width at half maximum of cross-scans obtained with the Urumqi and Effelsberg radio telescopes, we can rule out this hypothesis.

Assuming θ_s to be of the order of milliarcseconds or smaller (see, e.g., Lazio et al. 2008 and Qian & Zhang 2001), the source must be regarded as pointlike, and the factor θ_s/θ_f in Eq. 1 and 2 can be substituted with 1. The constraint on the variability time scale would require $v \leq 10^{-2}$ km s^{-1}. This is three orders of magnitude lower than the Earth's orbital velocity, which, reasonably, should provide a lower limit to v.

Looking at the literature, it is well known that InterPlanetary Scintillation (IPS) does contribute to the variability of compact radio sources (Readhead 1971). IPS causes variations of the scintillation index (the standard deviation of the flux density over an ensemble of measurements; it is equivalent to m_i) which depend on solar elongation. The effect is most prominent at low observing frequencies. Following Readhead 1971, for ϵ between ∼ 3° and ∼ 90°, and for frequencies between 81.5 MHz and 2.7 GHz, in the regime of weak scattering, the dependence of m_i on $\sin \epsilon$ and the frequency ν can be described as a power law

$$m_i(\nu) \, \nu \propto (\sin \epsilon)^{-1.55} \tag{5}$$

Extrapolating this result to a frequency of 4.8 GHz, and using a proportionality factor of 0.22 (see Readhead 1971) gives for sources with $\epsilon < 30°$ a m_i of the order of 1-10%, which is consistent with our results. The time scale of IPS variations, however, is of the order of seconds, at least 10^4 times smaller than the ones which characterize the Urumqi light curves.
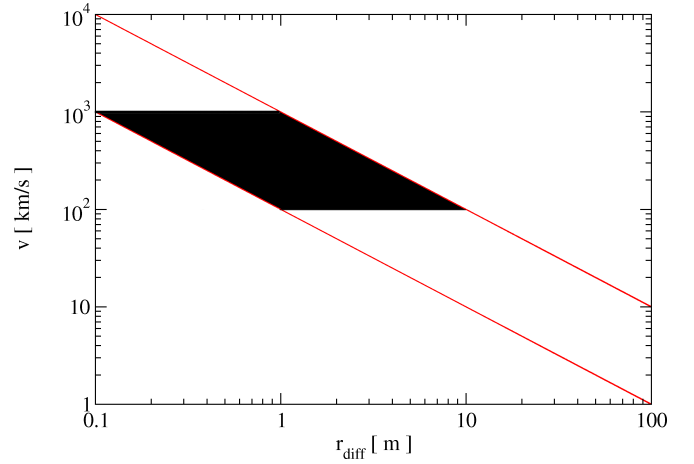
Fig. 8. Between the red lines, the range of values r_{diff} (x-axis) and v (y-axis) which are consistent with the variability characteristics observed in the Urumqi data. In black, the subset of values in the v-range 10^2–10^3 km/s, corresponding to the solar wind speed.

4.2. Strong scattering: refractive scintillation

Let us hypothesize that the variability is due to refractive scintillation. In the case of extended sources, the time scale and modulation index of the variability would be

$$\tau_{ref} \approx \frac{r_{ref}}{v} \frac{\theta_s}{\theta_{scatt}} \tag{6}$$

and

$$m_{i,ref} \approx \left(\frac{r_{diff}}{r_f}\right)^{1/3} \left(\frac{\theta_{scatt}}{\theta_s}\right)^{7/6} \tag{7}$$

where $r_{ref} = r_f^2/r_{diff}$ and $\theta_{scatt} = r_{ref}/D$. The factor θ_s/θ_{scatt} can be replaced with 1 in the case that $\theta_s < \theta_{scatt}$. Considering that $\theta_{scatt} > \theta_f$, we can assume this condition to be true when dealing with interplanetary scintillation of compact radio sources. Using Eq. 6 and 7, we calculated the values of v and r_{diff} which are consistent with the observed variability characteristics (a modulation index of a few percent and $\tau_c \sim 10^4$–10^5 s). They are plotted in Fig. 8. The range of values which are consistent with the solar wind speed are marked in black. It appears that in order to explain the detected variability by means of refractive scintillation we must hypothesize the existence of density inhomogeneities in the solar wind on a spatial scale of tens of meters or less. Previous studies (see, e.g., Narayan et al. 1989 and Coles et al. 1991), refer to an inner scale of turbulence of the order of kilometers.

4.3. Scattering in the Earth's bow shock

The sharp increase in the fractional modulation index at solar elongation close to 30° is compatible with another hypothesis, namely that the variability increases due to propagation effects in the region where the solar wind and the Earth's magnetosphere meet, i.e. the Earth's bow shock. Here the solar wind speed drops considerably due to the interaction with the Earth's magnetic field. It is worthwhile to investigate what values of v and r_{diff} would be required to explain the variability characteristics we found, considering a screen at a distance of ∼ 10^8 m, consistent with the approximative distance to the bow shock. This results in a Fresnel scale of ∼ 10^3 m and a Fresnel angle of the order of

arcseconds, which implies that all the sources can be treated as pointlike. In the case of weak scattering, a variability time scale of $\sim 10^4$ s leads to a velocity v of the order of a few m/s — very low, even for the bow shock — while from a modulation index of the order of 1% we can deduce $r_{diff} \sim 10^5$ m. For refractive scintillation, instead, the constrains on m_i and τ_c would lead to $r_{diff} \simeq$ m and, consequently, $v \sim 10^2$ km/s. The value of r_{diff}, in this case, is much smaller than we would expect.

### 4.4. Correlation between short- and long-term variability

As shown above, both the hypotheses of weak and strong (refractive) scattering can hold only assuming either a very slow moving component of the solar wind or irregularities in the interplanetary plasma on very small size scales. For typical parameters of the interplanetary plasma, instead, IPS should cause variability on time scales of seconds. Since the Urumqi observations are performed through sub-scans which have a duration of about 30 seconds, an IPS effect would likely appear as an additional noise superimposed to the Gaussian profile of the flux density measurements. An increase in the noise caused by IPS should translate into a larger uncertainty in the flux density measurement.

For all the observing sessions, we estimated the mean error on the flux density measurements derived from the single sub-scans. The aim was to check if the variations in the modulation index could be associated to similar variations in the flux density measurement error. Note that in the error estimation there is a component which depends on the flux density. Such a component can vary considerably for a strongly variable source such as AO 0235+164 and must be removed. We used the calibrators to derive the proportionality factor, α_n, between the flux density (S) and the error (ΔS). The flux-independent error for AO 0235+164 was estimated as $(\Delta S)' = \Delta S - \alpha_n S$. The results are presented in the upper panel of Fig. 9. The cyan dots show the ratio between the errors and the average flux density of AO 0235+164 calculated over the ~ 3 years of observation, expressed in percentage. This is meant to give an estimation of the contribution of flux-independent error to the measurement uncertainty. Such a contribution is small compared to the variability on longer time scales, estimated through the modulation index (black dots in Fig. 9). However, a locally normalized discrete correlation function (see Edelson & Krolik 1988, Lehar et al. 1992) between the two parameters shows a very high degree of correlation (Fig. 9, lower panel), higher than 0.9. Remarkable are also the peaks of correlation for time lags of ±1 and ±2 years, which confirm the one-year periodical nature of the variations in both the parameters.

Let us hypothesize that the measurement error directly affects the modulation index by introducing uncorrelated noise in the flux density estimation, due to the uncertainty in the measurements. The periodic increase in the modulation index would correspond to an equivalent increase in the contribution of uncorrelated noise to the overall variability. This, however, is not the case. Since uncorrelated noise has a time scale which must be of the order of the average sampling of the light curves, it can be isolated by separating the very fast variability from the slow one throughout a de-trending procedure (see Villata et al. 2002). The variability amplitude of the de-trended data (red triangles in Fig. 9, upper panel) provides us with an upper limit to the contribution due to the measurement uncertainty. The comparison between the modulation index of the de-trended light curves and the ones of the long-term trends (green squares in Fig. 9, upper panel) demonstrates that the measurement uncertainty plays a
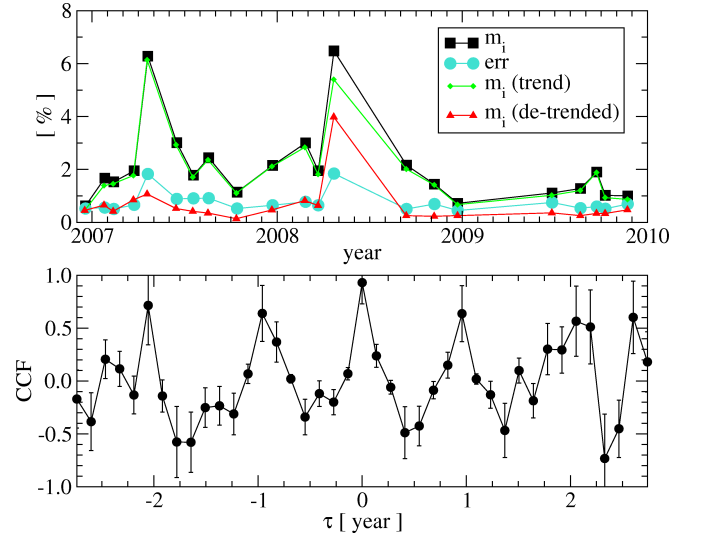
Fig. 9. Upper panel: the modulation index (black dots) and the average flux density measurement errors (cyan dots) of AO 0235+164 plotted versus time. The errors are given in percentage with respect to the average flux density of the source during the ~ 3 years of observation. The green squares and red triangles show the modulation index of the slow and of the fast variability component, respectively. Lower panel: the correlation function between the modulation index and the flux density measurement errors.
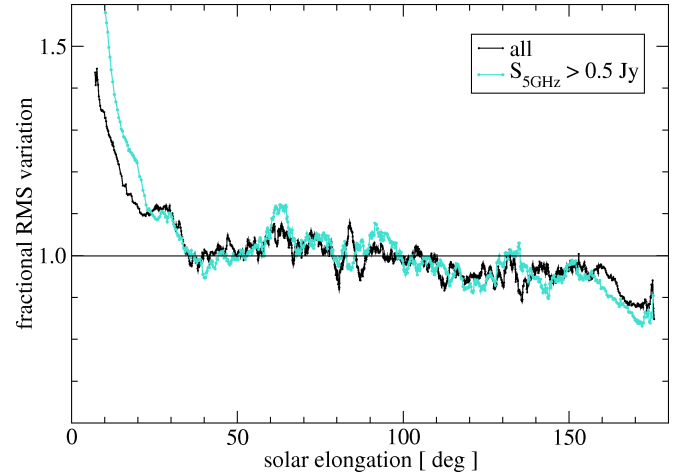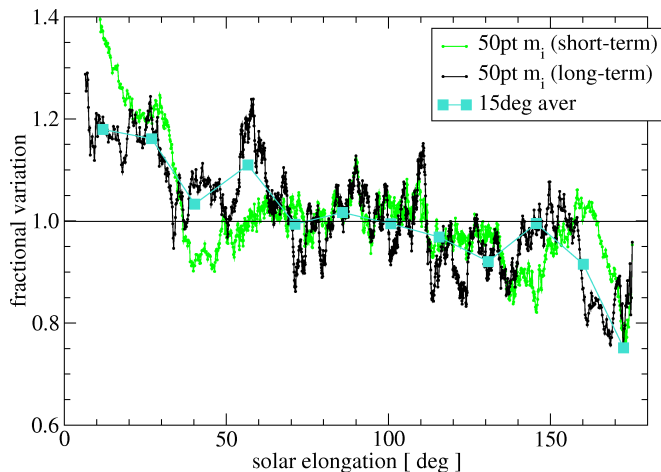

Fig. 10. The 50-point running averages of the fractional RMS of the error-in-the-mean for all the MASIV sources (black line) and for a sub-sample of strong sources (cyan line). The solar elongation dependence is more pronounced in the latter ones.

marginal role for the total variability, except maybe for the cases of the December 2006 and April 2008 observing sessions. Once we excluded that the measurement error directly affects the modulation index, we can conclude that the correlation between the two is due to a common origin of their variations.

Concerning the MASIV data, possible variability on IPS time scales may be investigated by looking at the RMS error-in-the-mean for each scan. This is calculated from the scatter in the visibilities over all sub-integration times (typically 18 per one-minute scan, H. Bignall, priv. comm.) and all baselines (typically 10). The RMS error-in-the-mean for all the scans were kindly provided by J. Lovell. Following the same approach as in Eq. 3, for each source we calculated the fractional RMS error-in-the-

Fig. 11. 50-point running averages of the fractional modulation index of both the long- (black line) and the short-term variability (green line) in the MASIV data. The cyan squares show a 15-degree average on the long-term data.

mean at each observing session, and we plotted it as a function of solar elongation. Its 50-point running average is shown in Fig. 10 (black line). The parameter follows a similar increasing trend as the modulation index, showing a prominent increase in the fractional variation for solar elongations ϵ below 35°. Remarkably, the solar elongation dependence of the RMS is more pronounced in the stronger MASIV sources ($S_{5GHz} > 0.5$ Jy, cyan line in the figure). Likely, while for low flux density sources the RMS scatter on very short time scales is mainly due to thermal noise and confusion, for strong sources it is dominated by IPS.

For each MASIV light curve, we separated the long-term trend (which carries information about the variability on time scales of one day or more) from the fast variability component, calculating the modulation index of both. We repeated the analysis presented in Fig. 6 for the trend and the de-trended data separately. The results, plotted in Fig. 11, show a strong solar-elongation dependence in the short-term variability (green line). A similar trend, weaker but still important, also appears in the long-term variability (black line), as a 15-degree average (cyan squares) clearly shows. This suggests that the influence of the Sun on the variability of compact sources goes far beyond the typical IPS time scales.

The hypothesis that the variability of AO 0235+164 is related to IPS is strengthened by the results discussed above. They can be summarized as follows: solar-elongation related variability on IPS time scales appears both in the Urumqi and in the VLA data. Looking at the Urumqi observations, we found evidence that this fast variability component correlates with the variability on typical IDV time scales. Still, to explain the phenomenon in terms of IPS we would need to postulate the existence of an *atypical*, long-term manifestation of IPS. A possible explanation would be that the variability on time scales of seconds do not introduce a random error in the flux density measurement. We could hypothesize that the scattering causes preferentially an underestimation of the flux density of the source, by increasing the opacity of the scattering medium. In this case, a stronger scattering — due to a more turbulent medium in proximity of the Sun — would lead to lower values of the measured flux density. Changes in the average conditions of the medium along the line-of-sight, which could reasonably take place on time scales of hours or more, or changes in the line-of-sight itself, would appear as a long-term trend in the light curve of the

source. A possible confirmation of this picture may come from the results of a study about extreme scattering events, reported by Lazio et al. (2001). Using the Green Bank Interferometer, the authors monitored 149 compact radio sources with an average sampling of about one data-point every two days. They found evidence for a remarkable decrease (10-20%) in the 2 GHz flux density of 0952+179 in two separate occasions. Both events happened when the source was at low solar elongation. The time scales of the variations was of the order of weeks, which would be compatible with the long-term manifestation of IPS hypothesized above. At 8 GHz frequency, however, the drop in flux density was not seen.

The existence of a correlation between slow and fast variability may also open the way to a completely different explanation. Observations performed close to the line-of-sight of the Sun may be strongly affected by atmospheric effects (e.g. turbulence in the ionosphere). These are usually ignored because of their short time scales, but if a connection between short and long time scale variability could be hypothesized in the case of the interplanetary medium, the same could also be valid for the atmosphere.

In section 3.3, we underlined that the Δm_{max} value obtained for AO 0235+164 from all the Urumqi observations (i.e. including the two April sessions) is much higher than the one obtained from the MASIV data. This could be caused by changes occurring either in the source structure or in the scattering screen during the few years which separate the experiments; but it could also be caused by the difference between the facilities, in the sense that the Urumqi telescope may be more sensitive to the effect than the VLA. This may point towards a possible technical problem. An obvious candidate would be the effect of solar radiation into the sidelobes of the telescope or the receiver. There are facts, however, which seem to rule out this hypothesis. If we repeat the analysis shown in Fig. 6 on sub-samples of strong and weak MASIV sources (with $S_{5GHz} > 0.5$ Jy and < 0.2 Jy, respectively; see Fig. 12) we find that the former are considerably more affected than the latter ones. This is consistent with the results concerning the RMS error-in-the-mean of the scans, discussed above. An additional contribution to the variability by the solar radiation should have appeared more clearly in the light curves of weak sources. Furthermore, the solar radiation would be expected to introduce flux density fluctuations which are comparable for sources of similar brightness. Instead, the large variations observed in the modulation index of AO 0235+164 do not appear in CTA 21, a steep-spectrum source which is only a few degrees away from AO 0235+164 and is similarly bright. Still at a solar elongation of ∼ 20°, the modulation index of CTA 21 is of the order of 0.5%.

Another possible technical problem which could affect flux density measurements and depend on solar elongation is the pointing error. Reporting about the discovery of flickering in compact radio sources, Heeschen (1984) specified that a considerable number of flux density measurements were excluded from the analysis because of the increase in the pointing errors at low solar elongations. We calculated the average pointing offsets for all the AO 0235+164 Urumqi observations. The April 2007 pointing offset turned out to be the second lowest in the time span between 2005 and spring 2007, when the pointing model of the telescope was changed. Concerning April 2008, the pointing offset is lower than the average one calculated between 2007 and 2010. This suggests that a pointing problem cannot account for the solar-elongation related variability observed in Urumqi.
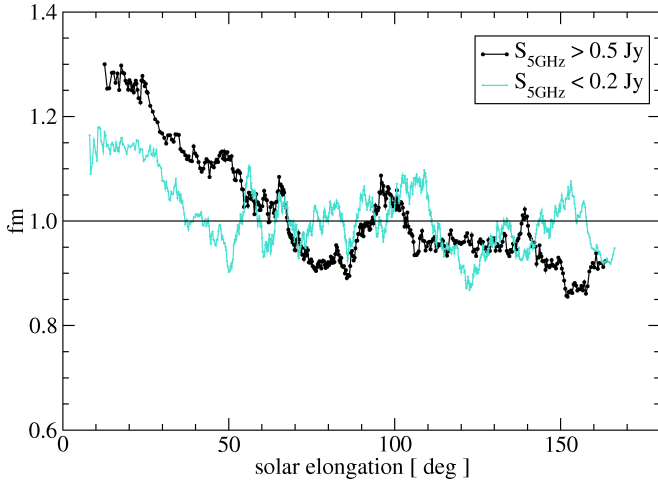
Fig. 12. Results of a 40-point running average on two subsets of MASIV sources. The black curve concerns sources with $S_{5GHz} > 0.5$ Jy, the cyan line sources with $S_{5GHz} < 0.2$ Jy. For strong sources the solar-elongation dependence of the variability is much more prominent than for weak sources.

4.5. The AO 0235+164 variability characteristics in April 2007 and 2008

The large difference between the characteristic time scales of AO 0235+164 in April 2007 and April 2008 deserves a final remark. While in the first epoch most of the variability is due to a slow component ($\tau_c \sim 2$ days), the April 2008 light curve is characterized by a variability time scale which is comparable to the average sampling (τ_c of the order of one hour, see Fig. 5). As already mentioned, this may indicate that the variability characteristics of the latter are dominated by the uncertainty on the flux measurements. The high amplitude variations observed in AO 0235+164 during the two epochs may be caused by effects which are correlated, but are not the same. Further observations are needed to understand at which solar elongation the fast variability component starts to dominate over the slow one, if and how this can be influenced by the activity of the Sun, and if the characteristics of the observing facility play a role in it.

It cannot be excluded that also the conditions in the source itself have to be taken into consideration. Differently from April 2008, in April 2007 AO 0235+164 was in a flaring state (see Raiteri et al. 2008). The ejection of a strong and very compact emitting component could have caused an additional variability contribution with characteristic time scale of ~ 2 days, due to ISS. The superposition of the variability contributions due to IPS and ISS could be the origin of the difference between the variability time scales in the two epochs.

5. Summary

This paper reports on the discovery of a seasonal cycle in the amplitude of the variability in the IDV source AO 0235+164 during the ~ 3 years of monitoring performed at the Urumqi Observatory. The variability peaks at the time of minimum solar elongation of the source, suggesting interplanetary scintillation as a possible cause of the phenomenon.

We performed a thorough investigation of the variability characteristics of a sample of 475 sources, provided by the MASIV survey, with the aim of establishing whether such a phenomenon generally enhances the variability of compact radio sources. This study led to the conclusion that solar-elongation

related variability provides a significant contribution to the total variability, especially for $\epsilon < 30°$. As expected, the effect is most prominent for sources at low ecliptic latitude. We estimate that for sources with $\beta \sim 0°$ the variability increases by a factor of two over the average source modulation index as they pass from the maximum to the minimum solar elongation. The findings of the present study may have important implications for future large-area sky monitoring surveys (e.g. the proposed ASKAP VAST Survey; see Chatterjee et al. 2010).

The nature of the variability is not yet completely understood. We took into consideration the hypothesis of weak scattering and strong scattering from refractive scintillation in the vicinity of the Sun as possible causes of the phenomenon. In the first case, a very slow component of the solar wind (with speed of the order of a 10 meters per second) would be needed to explain the observed variability characteristics. The refractive scintillation model, instead, implies the existence of very small structures in the interplanetary plasma. These conditions seem doubtful and do not find confirmation in previous studies in the literature. We also took into consideration the hypothesis that the change of variability is due to propagation effects in the Earth's bow shock. The deduced values of v and r_{diff} are not consistent with the expected ones.

We hypothesize that a change in the average parameters of the solar wind along the line-of-sight to the sources may provide a possible explanation for the long time scale of the observed variability.

The strong correlation found in the Urumqi data between the measurement error on single sub-scans and modulation index may be evidence of a link between IPS (whose variability time scale is comparable with the duration of a sub-scan) and the long-term variability. A similar kind of investigation carried out on the MASIV data seems to support this idea. However, alternative interpretations in terms of an *indirect* effect of the Sun, atmospheric or even telescope-related effects cannot be excluded. To discriminate between the different hypotheses, further investigations are needed.

References

Bignall, H. E., Jauncey, D. L., Lovell, J. E. J. et al. 2003, ApJ, 585, 653
Chatterjee, S., Murphy, T., & VAST Collaboration 2010, Bulletin of the American Astronomical Society, 42, 515
Coles, W. A., Liu, W., Harmon, J. K. & Martin, C. L. 1991, J. Geophys. Res., 96, 1745
Dennett-Thorpe, J., & de Bruyn, A. G. 2000, ApJ, 529, L65
Dennett-Thorpe, J., & de Bruyn, A. G. 2002, Nature, 415, 57
Edelson, R. A., & Krolik, J. H. 1988, ApJ, 333, 646
Gabányi, K. É., Marchili, N., Krichbaum, T. P. et al. 2007, A&A, 470, 83
Heeschen, D. S. 1984, AJ, 89, 1111
Heeschen, D. S., Krichbaum, T., Schalinski, C. J., & Witzel, A. 1987, AJ, 94, 1493
Kraus, A. 1997, Ph.D. Thesis, Bonn University, Germany
Kraus, A., Quirrenbach, A., Lobanov, A. P. et al. 1999, A&A, 344, 807
Lazio, T. J. W., Waltman, E. B., Ghigo, F. D., et al. 2001, ApJS, 136, 265
Lazio, T. J. W., Ojha, R., Fey, A. L., et al. 2008, ApJ, 672, 115
Lehar, J., Hewitt, J. N., Burke, B. F., & Roberts, D. H. 1992, ApJ, 384, 453
Lomb, N. R. 1976, Ap&SS, 39, 447
Lovell, J. E. J., Jauncey, D. L., Bignall, H. E., et al. 2003, AJ, 126, 1699

Lovell, J. E. J., Rickett, B. J., Macquart, J.-P. et al. 2008, ApJ, 689, 108
Marchili, N., Krichbaum, T. P., Liu, X., et al. 2008, arXiv:0804.2787
Marchili N. 2009, Ph.D. Thesis, Bonn University, Germany
Marchili, N., Martí-Vidal, I., Brunthaler, A., et al. 2010, A&A, 509, A47
Narayan, R., Anantharamaiah, K. R. & Cornwell, T. J. 1989, MNRAS, 241, 403
Narayan, R. 1992, Royal Society of London Philosophical Transactions Series
    A, 341, 151
Qian, S.-J. & Zhang, X.-Z. 2001, Chinese J. Astron. Astrophys., 1, 133
Quirrenbach, A., Witzel, A., Wagner, S., et al. 1991, ApJ, 372, L71
Quirrenbach, A., Witzel, A., Krichbaum, T. P., et al. 1992, A&A, 258, 279
Raiteri, C. M., Villata, M., Larionov, V. M., et al. 2008, A&A, 480, 339
Readhead, A. C. S. 1971, MNRAS, 155, 185
Rickett, B. J., Witzel, A., Kraus et al. 2001, ApJ, 550, L11
Rickett, B. J., Lazio, T. J. W., & Ghigo, F. D. 2006, ApJS, 165, 439
Scargle, J. D. 1982, ApJ, 263, 835
Senkbeil, C. E., Ellingsen, S. P., Lovell, J. E. J., et al. 2008, ApJ, 672, L95
Simonetti, J. H., Cordes, J. M., & Heeschen, D. S. 1985, ApJ, 296, 46
Sun, X. H., Reich, W., Han, J. L., et al. 2006, A&A, 447, 937
Villata, M., Raiteri, C. M., Kurtanidze, O. M., et al. 2002, A&A, 390, 407
Wagner, S. J., & Witzel, A. 1995, ARA&A, 33, 163
Witzel, A., Heeschen, D. S., Schalinski, C., & Krichbaum, T. P. 1986,
    Mitteilungen der Astronomischen Gesellschaft Hamburg, 65, 239